Exceptional service in the national interest

Sandia National Laboratories

TMS 2023 Annual Meeting – March 19-23, 2023

Additive Manufacturing

Length-Scale Phenomena in Mechanical Response: Modeling

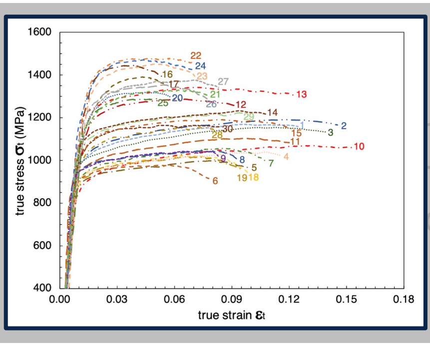

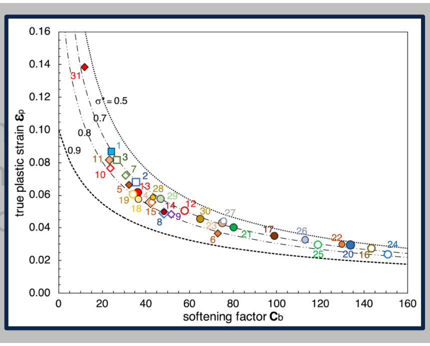

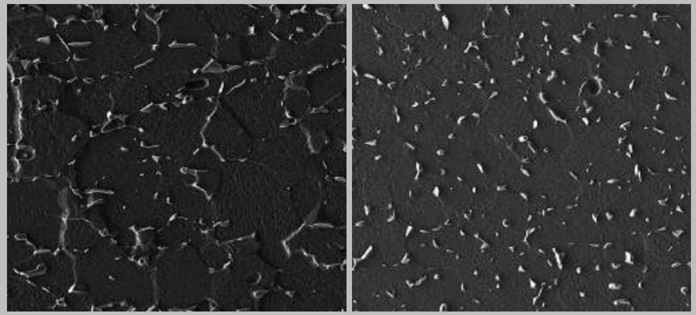

Analytic model for the softening factor within stages of work hardening

Alan F. Jankowski

U.S. DEPARTMENT OF ENERGY

NNSA National Nuclear Security Administration

Sandia National Laboratories is a multimission laboratory managed and operated by National Technology and Engineering Solutions of Sandia, LLC, a wholly owned subsidiary of Honeywell International, Inc., for the U.S. Department of Energy's National Nuclear Security Administration under contract DE-NA0003525.

SAND2023-abcd C

Motivation

- To develop the application of a work-hardening model that provides *a constitutive parameter* which characterizes the underlying microstructural scale for materials –
  - having a wide-range in tensile behavior, i.e. strength and ductility
  - being considered for structural applications – as steels and titanium alloys
  - having undergone rapid thermal transients during fabrication
  - containing anisotropic microstructures with submicron features
- Materials processed through various *additive manufacturing* (AM) methods are ideal candidates to assess
  - the tensile behavior of Ti-6Al-4V is analyzed from a literature survey for test results of materials produced by various AM methods

Background

- A constitutive model proposed by J.W. Morris, Jr. (2007) provides a means to compute a *softening factor* c_b that provides insight to the microstructural scale which is responsible for the plasticity during work hardening
  - the model was used to predict the amount of plasticity that can be obtained from a two-phase structure in nano steels up to the strength instability
  - the plastic strain ε_p can be computed between the proportional limit σ_y and strength σ_u at the instability as determined through the subtangent method of the Considère criterion, where the work-hardening rate Θ equals $d\sigma/d\varepsilon$
- The model was developed by Jankowski, et al. (2019, 2020, 2021) to assess the changes in structure and mechanical behaviors that are commensurate with AM process variants and post processing treatments
  - *details of work hardening stages are now assessed with respect to: the Voce stress-strain mechanism; and provide insight to the initiation of plastic deformation*

The softening factor c_b

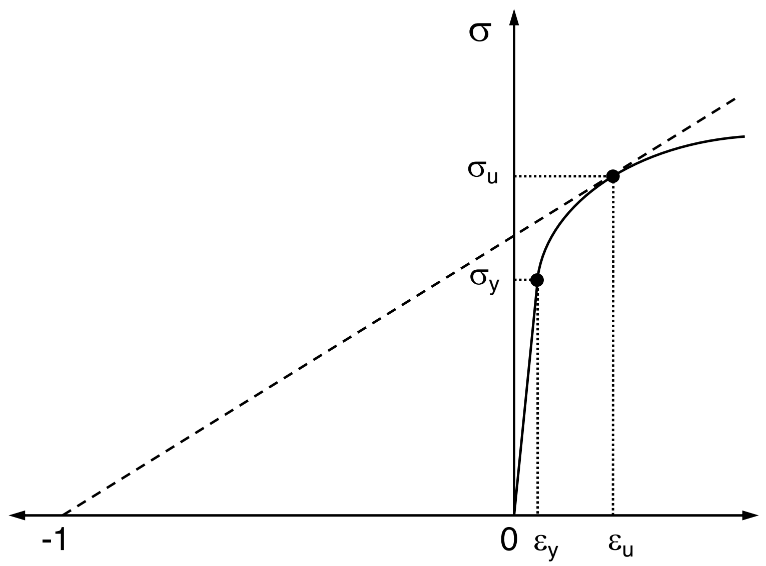

- The subtangent construct of the Considère criterion

  $d\sigma/d\varepsilon = \sigma/(1+\varepsilon)$ (1)

  where the instability is determined when

  $\Theta_u = [d\sigma/d\varepsilon]_u = \sigma_u$ (2)

- Derivative to the Voce stress-strain relationship of $\sigma_v = c_1 \cdot [1 - c_2 \cdot e^{-c_3 \cdot (\varepsilon - \varepsilon_o)}]$ is the linear form of the Kocks-Mecking relationship where c_3 equals c_b

  $\Theta = \Theta_o - c_b \cdot \sigma$ (3)

- The true strain ε to the strength instability is determined by evaluating the eqn. (4) integral using eqns. (2-3), from σ_y to σ_u to arrive at eqn. (5) where $\sigma_y^* = (\sigma_y/\sigma_u)$

  $\varepsilon = \int (d\varepsilon/d\sigma) \cdot d\sigma = \int [\Theta(\sigma)]^{-1} \cdot d\sigma$ (4)

  $\boldsymbol{\varepsilon_p} = (\boldsymbol{c_b})^{-1} \cdot \ln[1 + \boldsymbol{c_b} \cdot (1 - \boldsymbol{\sigma_y^*})]$ (5)

Materials

- Ti-6Al-4V microstructure is affected by the AM deposition method and heat treatment
  - AM synthesis methods are
    - LDED – laser-based directed energy deposition
    - EBM – electron beam melting
    - SLM – selective laser melting
    - DMLS – direct metal laser sintering
  - Two types of microstructure are typical
    - EBM produces an α-phase lamellar structure
    - SLM produces an α'-phase martensite that transforms to $\alpha+\beta$ structure after heating, where the β-phase aligns with the build plate direction

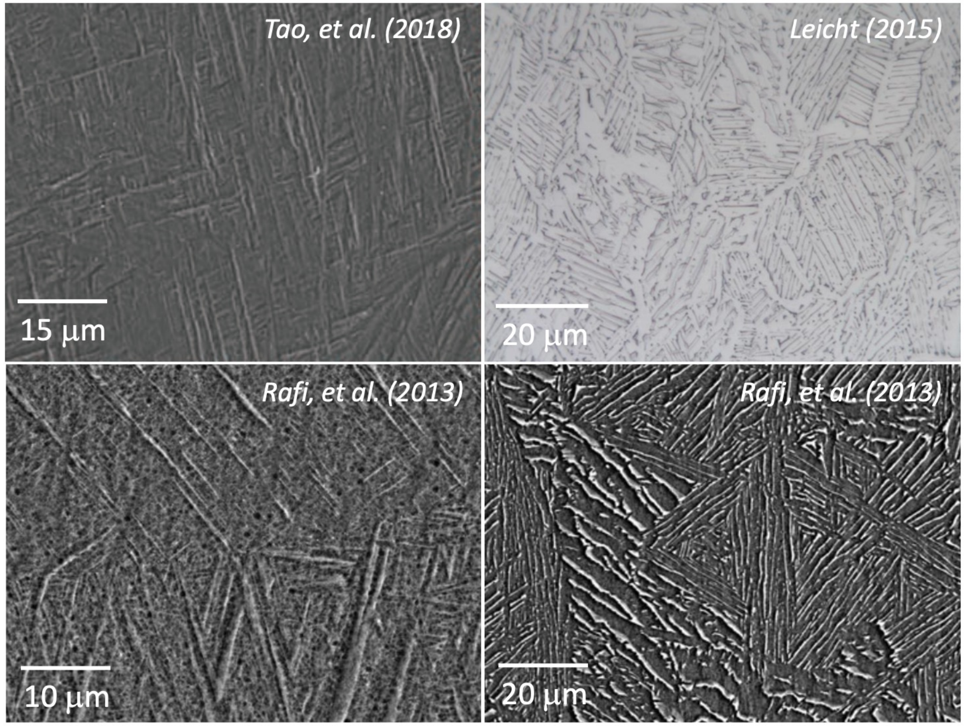

as-deposited SLM *as-deposited EBM*

Tensile tests

- Quasi-static strain rates from 10^{-5} to 10^{-3} s^{-1}
  - rate sensitivity effects are minimal
- Cylindrical and flat tensile bars are tested in both as-deposited and after heat treatments
  - stress-strain curves are digitized from literature reports
  - data is displayed to 3% beyond the instability
- Various orientations are selected from the build plates to include effects of anisotropy

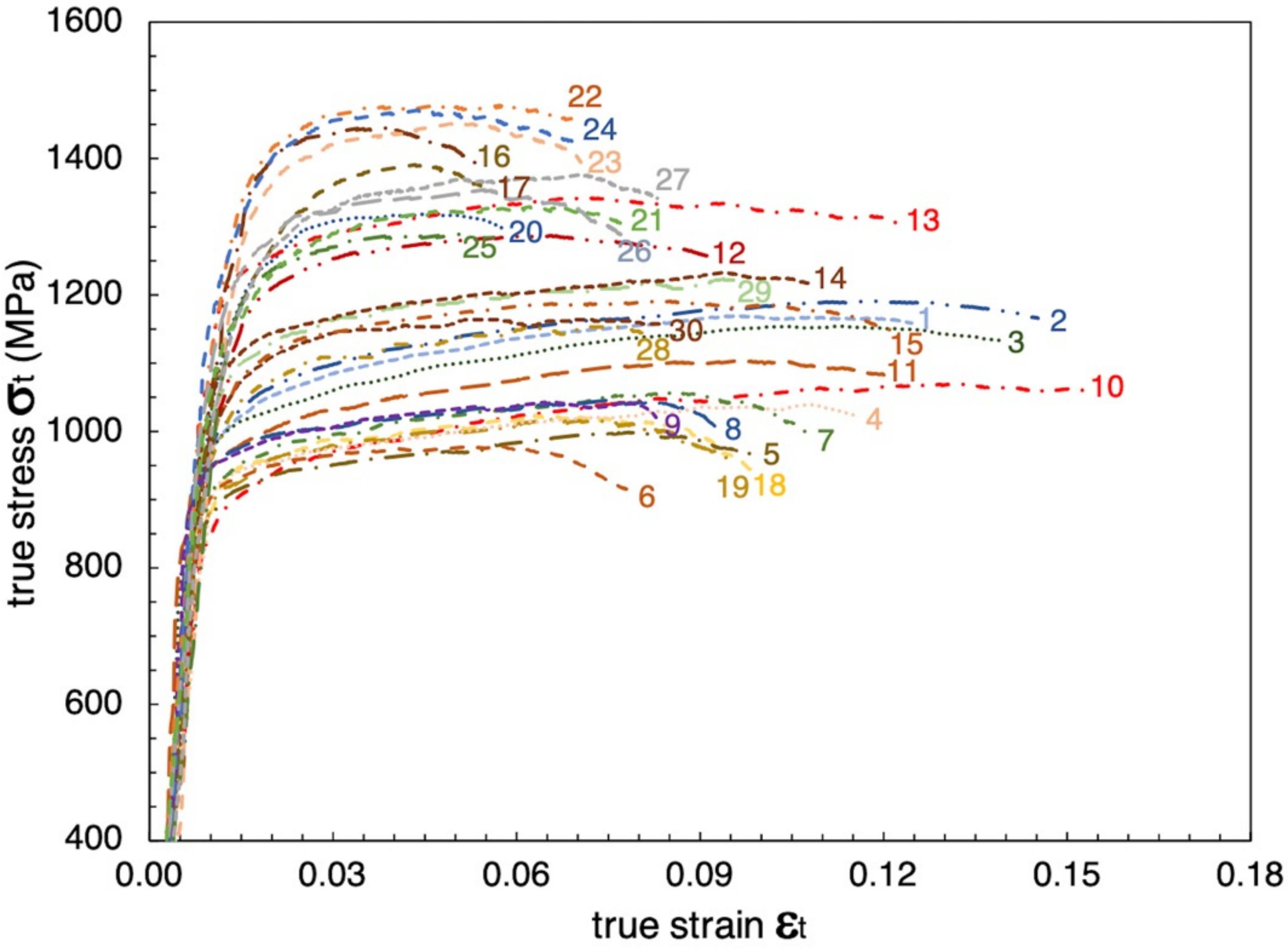

Table 1 – Results of tensile test analysis and AM sample information

no.	method	σ_u (MPa)	ε_p	σ^*	c_b	orientation	condition	reference
1	LDED	1168	0.087	0.70	24	z	as-printed	Carroll, et al. (2015)
2		1164	0.068	0.71	36	x-y (lower z)		
3		1140	0.081	0.71	27	x-y (upper z)		
4	EBM	1014	0.056	0.77	42	z	machined	Rafi, et al. (2013)
5		996	0.067	0.77	32			
6		972	0.037	0.81	73			
7		1052	0.072	0.73	31	x-y		
8		1035	0.049	0.80	48			
9		1035	0.048	0.79	52			
10		1047	0.076	0.78	24	x-y	as-printed	Leicht (2015)
11		1101	0.082	0.76	23	z		
12	SLM	1285	0.051	0.70	58	x-y		
13		1341	0.062	0.77	37	z		
14		1201	0.050	0.79	48	z	as-printed and HT	
15		1187	0.056	0.77	43	x-y		
16		1443	0.027	0.66	144	x-y	machined	Tao, et al. (2018)
17		1389	0.035	0.70	99	z		
18		1021	0.057	0.80	37	z	machined and HIP	
19		1015	0.061	0.80	34	x-y		
20		1312	0.029	0.64	134	-	-	Gorsse, et al. (2017)
21		1320	0.040	0.70	81	x-y	machined	He, et al. (2018)
22		1474	0.029	0.66	130	z	as-printed	Voisin, et al. (2018)
23		1448	0.043	0.68	75	z		
24		1460	0.024	0.76	151	x-y		
25		1283	0.030	0.73	119	x-y		
26		1339	0.033	0.66	113	z		
27		1367	0.044	0.64	76	x-y		
28	DMLS	1149	0.059	0.73	43	z	machined	Fadida, et al. (2018)
29		1205	0.058	0.70	47			
30		1164	0.045	0.73	65			
31	wire	1025	0.138	0.65	12	z	hot drawn	Jankowski, et al. (2019)

Sandia National Laboratories

Notes on results

- $\sigma^* = 0.74 \pm 0.06$ for all Ti-6Al-4V AM samples
  - $\sigma^* = 0.51 \pm 0.06$ was found for AM LPBF 316L
- elastic loading is consistent with a 114 GPa elastic modulus.
  - use $R^2 > 0.995$ to define linear elastic loading and to determine the proportional limit

Model analysis

- Plasticity ε_p is enhanced as the c_b-value decreases at constant σ^*
- Synthesis predictably affects strength
  - e.g. a higher strength of SLM martensitic structure in comparison to EBM α-phase lamellar structure
- No distinguishing effects for build orientation, or machined vs. as-printed surface finish of LM samples
- Post-deposition HIP treatment of SLM material does reduce
  - strength σ_u at the instability from 1415 to 1017 MPa (see no. 16-17 vs. 18-19)
  - c_b values from an average of 121 to just 34, with values now comparable with the average of 41±17 for all EBM samples

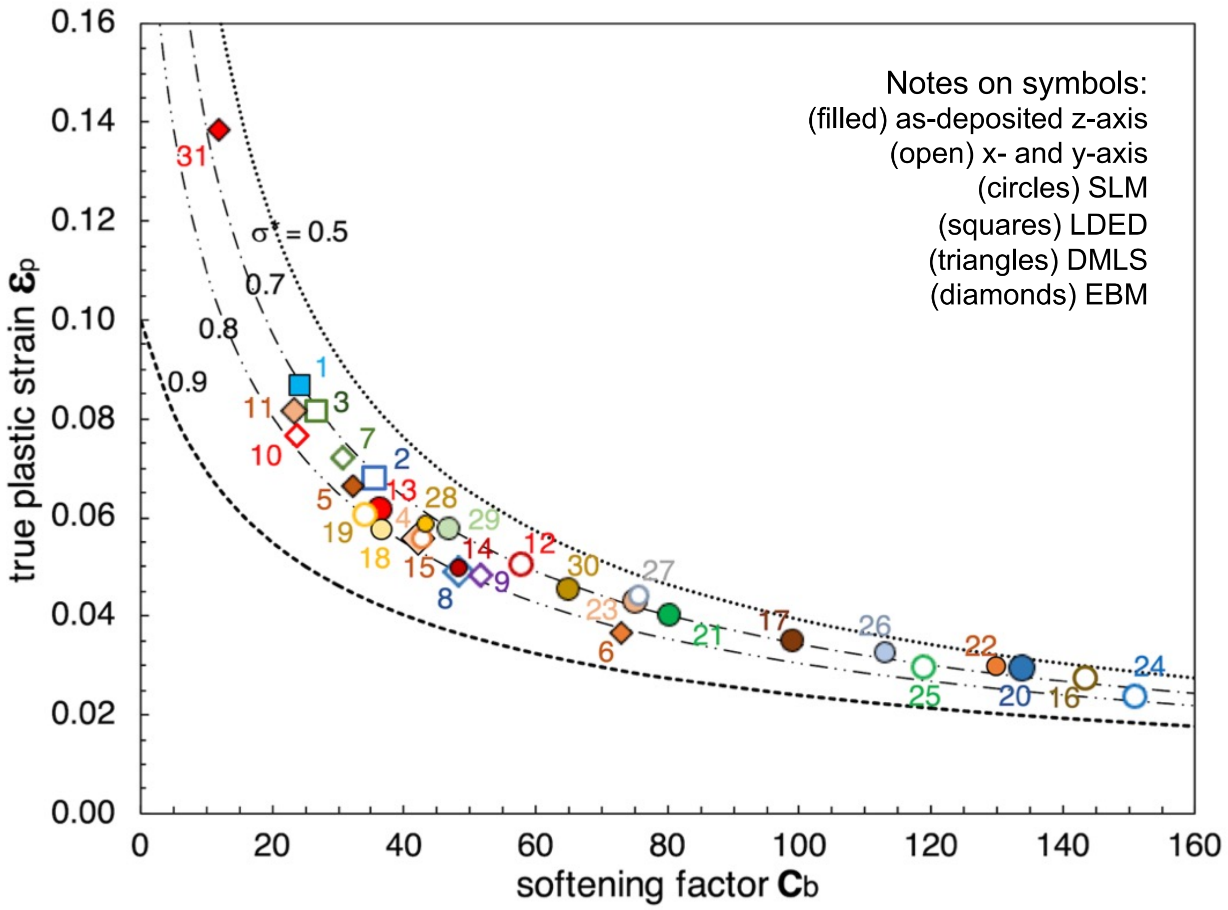

Kocks-Mecking (K-M) behavior

- The integral form of the derivation

  $\boldsymbol{\varepsilon_p} = (\mathbf{c_b})^{-1} \cdot \ln[1 + \mathbf{c_b} \cdot (1 - \boldsymbol{\sigma_y}*)]$ (5)

  provides a unique c_b value for a linear stage of work hardening

  $\Theta = \Theta_o - \mathbf{c_b} \cdot \sigma$ (3)
- However, the K-M plot (right) shows two distinct linear regions – a steep linear decrease in $\Theta(\sigma)$, followed by a shallow decay during the extended range of plasticity – for which c_b dominates
- Consideration is now given to formulate expressions for these distinct stages of work hardening

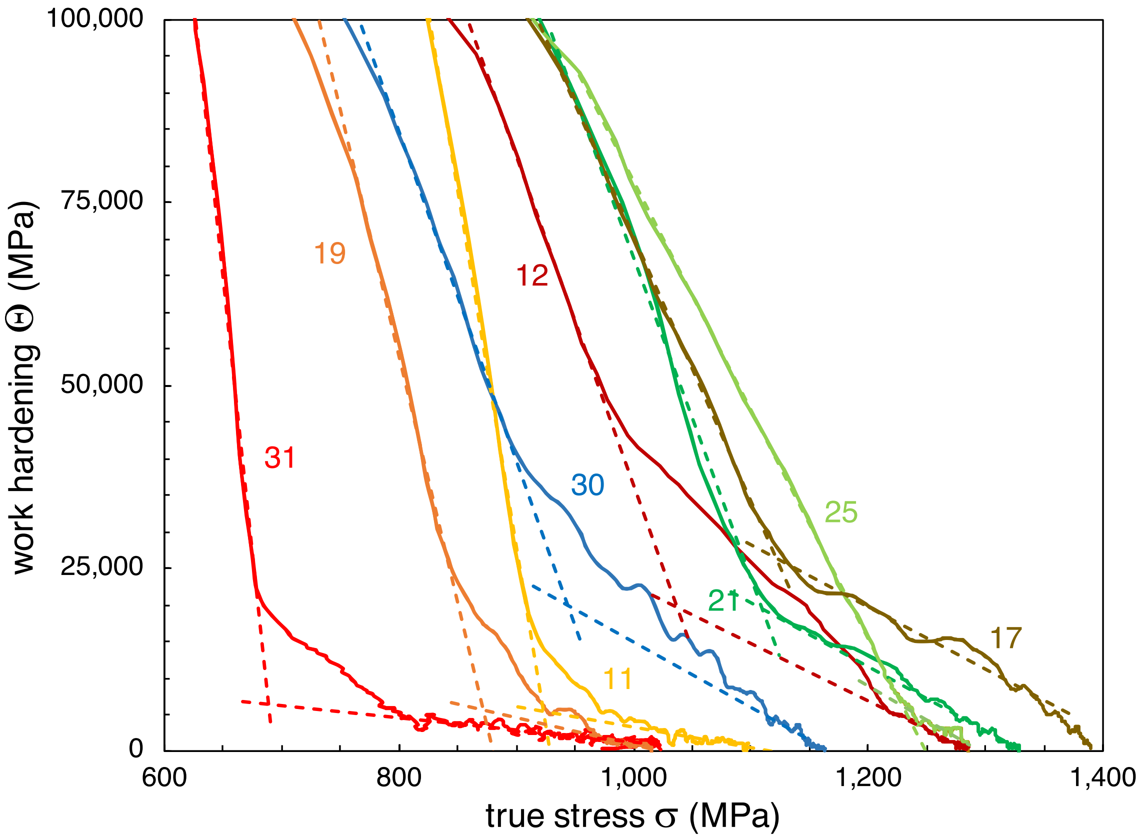

Formalisms for stages 3 and 4

- From the idealized behavior (shown right), the sequential stages 3 and 4 can be expressed as

  $\Theta_3 = \Theta_{o3} - \mathbf{c_{b3}} \cdot \sigma$ (6a)

  $\Theta_4 = \Theta_{o4} - \mathbf{c_{b4}} \cdot \sigma$ (6b)

  where the corresponding formulations for strain are

  $\varepsilon_3 = (c_{b3})^{-1} \cdot \ln[(\Theta_{o3} - c_{b3} \cdot \sigma_y)/(\Theta_{o3} - c_{b3} \cdot \sigma_d)]$ (7a)

  $\varepsilon_4 = (c_{b4})^{-1} \cdot \ln[(\Theta_{o4} - c_{b4} \cdot \sigma_d)/(\sigma_u)]$ (7b)

  and the stress intercept $\sigma_d = (\Theta_{o3} - \Theta_{o4})/(c_{b3} - c_{b4})$
- The $\mathbf{c_{bi}}$ values are computed with eqns. (7a-7b) using the plastic strain between each increment of stress, i.e. from σ_y to σ_d, and from σ_d to σ_u

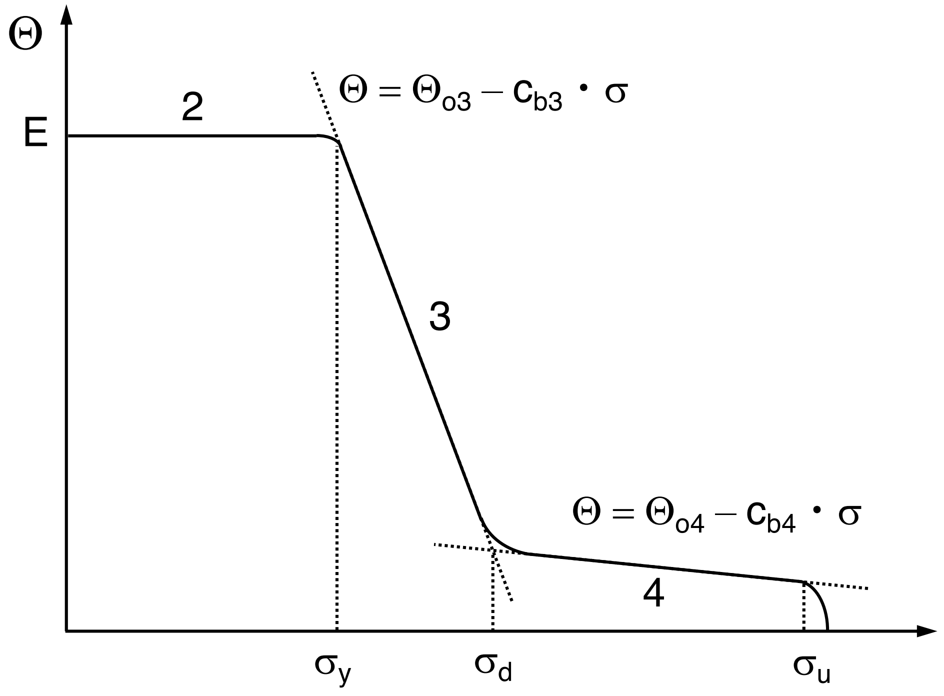

Results for stages 3 and 4

- The down-selection of samples for analysis is now made to represent a broad range of c_b-values
- The c_b and c_{b4} values are quite similar, and represent the majority of plastic deformation where $\varepsilon_4 \leq \varepsilon_p$
- The c_{b3} values are much greater and sequence in reverse order to the c_{b4} values with respect to ε_i

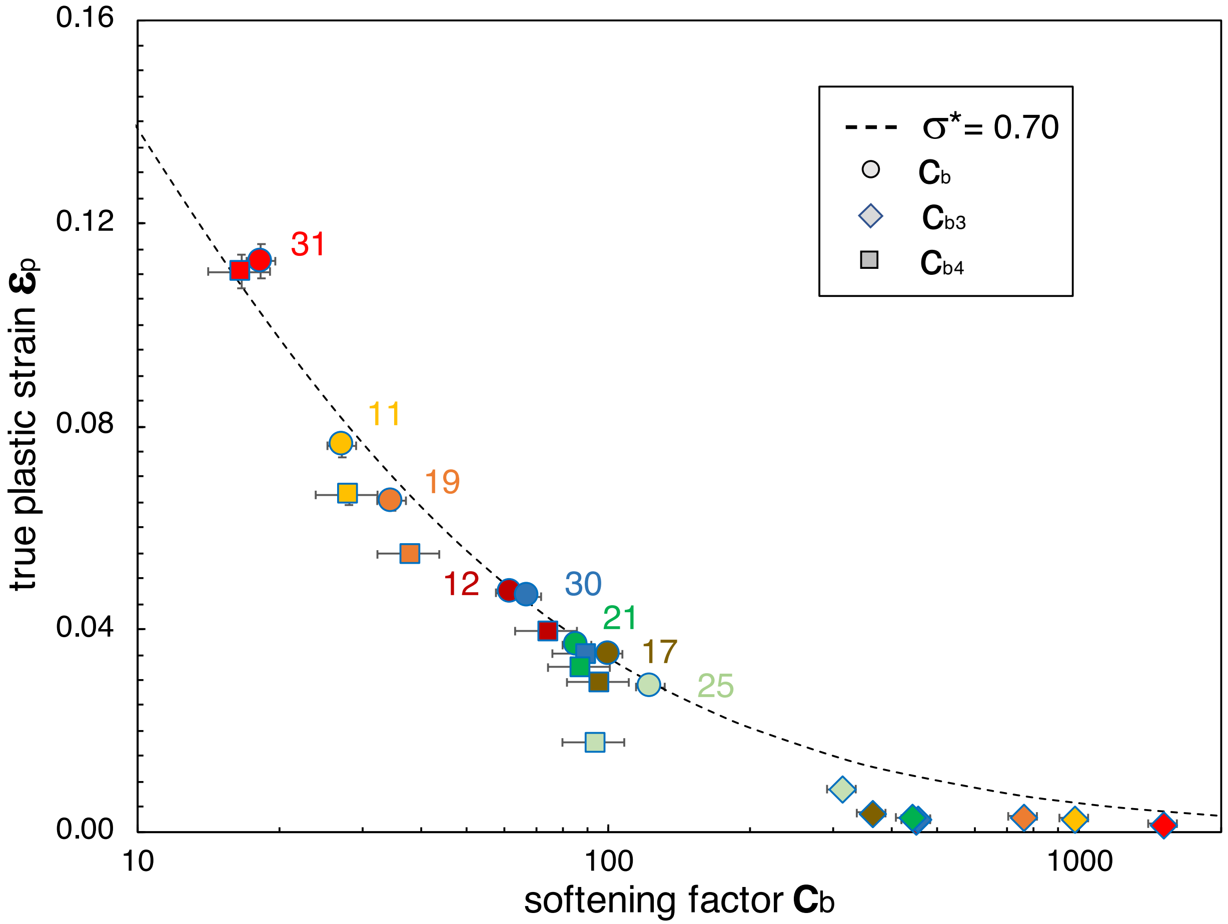

Stage 3 – Onset of plastic deformation

- The initiation of plastic deformation, at a strain rate $\dot{\varepsilon}$, occurs at the beginning of stage 3 by activating a volume of dislocations ν^* (e.g. Gibbs 1969) equal to

$$\nu^* = k_B \cdot T \cdot [\partial(\ln \dot{\varepsilon})/\partial(\sigma)] \qquad (8)$$

- Equation (8) can be expressed incorporating the Dorn relationship, using the strain rate sensitivity of strength **m**, as

$$\nu^* = k_B \cdot T \cdot (\mathbf{m} \cdot \sigma)^{-1} \qquad (9)$$

- Next, eqn. (9) is solved for σ and substituted into eqn. (6a) – the stage 3 expression for Θ_3 as

$$\Theta_3 = \Theta_{o3} - [(k_B \cdot T) \cdot c_{b3}/(m \cdot \nu^*)] \qquad (10)$$

- Equation (10) can be reduced to solve for ν^*, noting that $\Theta_3 = \Theta_2 = E$ at the outset of stage 3, and introducing a coefficient $\mathbf{c_{\nu*}}$ equal to $(k_B \cdot T)/(\Theta_{o3} - E)$ as

$$\nu^* = \mathbf{c_{\nu*}} \cdot (\mathbf{c_{b3}} / \mathbf{m}) \qquad (11)$$

Activation volume variation ν^* with c_{b3}

- An average activation volume ν^* of 0.35±0.04 nm^3 is determined from eqn. (11) using a strain-rate sensitivity exponent m of 0.014
  - This average volume equals 44.2±4.5 (b^3) dislocations using a 0.2 nm magnitude for the Burgers vector (b)
- The computed activation volume ν^* does decrease (as shown right) from the sample with lowest proportional limit (and greatest plasticity to the instability) to that with the greatest proportional limit (and least plasticity to the instability)

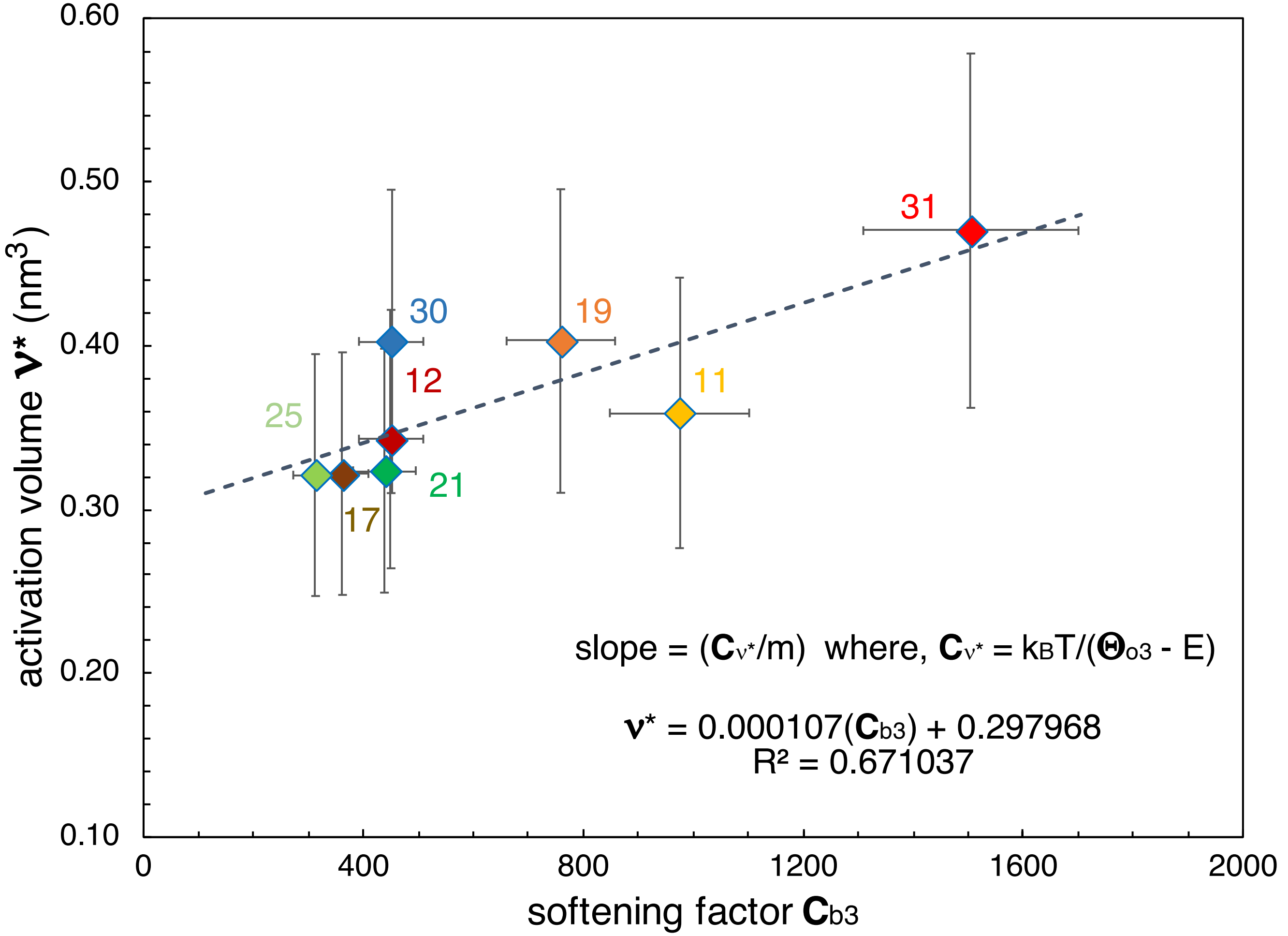

Simulating Voce behavior

- The linear regions of the K-M plot can be used to reconstruct the Voce stress-strain relationship (as shown for these curves), thereby providing a qualification proof of the c_b-method

  $c_1 = \Theta_{oi}/c_3$

  $c_2 = [1 - (\sigma_d/c_1)]\cdot e^{c_3\cdot\varepsilon}$

  $c_3 = c_{bi}$

- The dashed line represent modeling for stages 3 and 4 with a transition at σ_d between the linear stages
  - the stress-strain behavior over stage 4 is well simulated
  - *the stage 3 behavior is better fitted with a simulation analysis based on the Hollomon expression (shown elsewhere)*

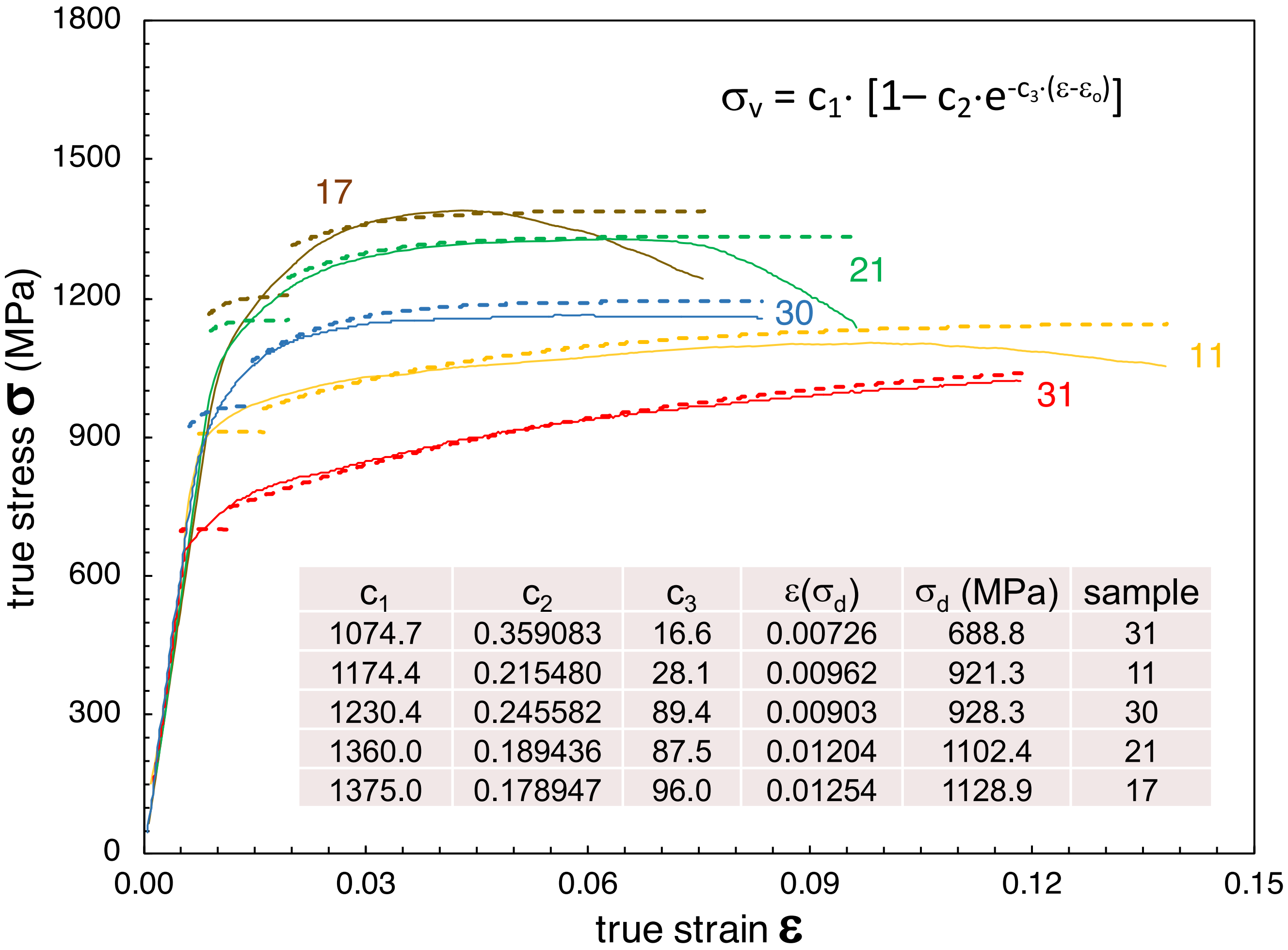

c_1	c_2	c_3	$\varepsilon(\sigma_d)$	σ_d (MPa)	sample
1074.7	0.359083	16.6	0.00726	688.8	31
1174.4	0.215480	28.1	0.00962	921.3	11
1230.4	0.245582	89.4	0.00903	928.3	30
1360.0	0.189436	87.5	0.01204	1102.4	21
1375.0	0.178947	96.0	0.01254	1128.9	17

Sandia National Laboratories

Summary

- A model by JW Morris, Jr. (2007) was developed that includes ε_p, σ_y and σ_u to define a softening coefficient c_b which provides a scale of microstructure attributable to the observed amount of work hardening
  - application was made for the behavior of Ti-6Al-4V produced by a variety of AM processes
  - a parametric evaluation, using c_b, was made of changes that occur with post-processing/aging
  - c_b-values decrease as the plastic strain ε_p increases, within an alloy representative σ^*-curve
- The approach is now developed to address the linear stages of K-M work hardening
  - c_{b3} values increase and the c_{b4} values decrease with an increase in total plastic strain ε_p
  - work hardening Θ_{o3}-values increase and Θ_{o4}-values decrease with an increase in ε_p
  - a formulation to determine the activation volume ν^* associated with the onset of plastic deformation is developed using stage 3 analysis – wherein, ν^*-values increase with c_{b3}
  - reconstructing a σ-ε curve from the work hardening plots validates the use of a Voce relationship in the K-M plot, especially for stage 4 as most of the work hardening is represented by a single integrated c_b coefficient

for further info – see Int J Mater Res. 110 (2019) 990; Mater Des Proc Comm. 2 (2020) e96 and 3 (2021) e262-1-9